INTERNATIONAL JOURNAL FOR NUMERICAL METHODS IN FLUIDS
Int. J. Numer. Meth. Fluids 2001; **37**: 721–745 (DOI: 10.1002/fld.197)

Comparisons of numerical methods with respect to convectively dominated problems

Yongqi Wang*,[1] and Kolumban Hutter[2]

Department of Mechanics, Darmstadt University of Technology, Darmstadt, Germany

SUMMARY

A series of numerical schemes: first-order upstream, Lax–Friedrichs; second-order upstream, central difference, Lax–Wendroff, Beam–Warming, Fromm; third-order QUICK, QUICKEST and high resolution flux-corrected transport and total variation diminishing (TVD) methods are compared for one-dimensional convection–diffusion problems. Numerical results show that the modified TVD Lax–Friedrichs method is the most competent method for convectively dominated problems with a steep spatial gradient of the variables. Copyright © 2001 John Wiley & Sons, Ltd.

KEY WORDS: convection; numerical method; total variation diminishing

1. INTRODUCTION

Successful modelling of strong convection is one of the most challenging problems in computational fluid mechanics. Although traditional first-order finite difference methods (e.g. first-order upstream and Lax–Friedrichs schemes) are monotonic and stable, they are also strongly dissipative, causing the solution to become smeared out and often grossly inaccurate. On the other hand, traditional high-order difference methods (e.g. central, second-order upstream, Lax–Wendroff, Beam–Warming, Fromm, QUICK, QUICKEST, etc.) are less dissipative but are susceptible to numerical instabilities, which cause non-physical oscillations in regions of large gradient of the variables. The usual way to deal with these types of oscillation is to incorporate artificial diffusion into the numerical scheme. However, if this is applied uniformly over the problem domain, and enough diffusion is added to dampen spurious oscillations in regions of large gradients, then the solution is also smeared out elsewhere.

* Correspondence to: Institut fur Mechanik III, Technische Universitat Darmstadt, Fachbereich 6, Hochschulstrasse 1, D-64289 Darmstadt, Germany.
[1] E-mail: wang@mechanik.tu-darmstadt.de
[2] E-mail: hutter@mechanik.tu-darmstadt.de

Received 8 June 2000
Revised 6 February 2001

In the past 20 years, tremendous amounts of research has been done in developing and utilizing modern high-resolution methods for approximating solutions of hyperbolic systems of conservation laws. Among these methods, the flux-corrected transport (FCT) method [1–6] and the total variation diminishing (TVD) schemes [7–10] are the most widely used discretization schemes of this sort.

The FCT technique is a scheme for applying artificial diffusion to the numerical solution of convectively dominated flow problems in a spatially non-uniform way. More artificial diffusion is applied in regions of large gradients, and less in smooth regions. The solution is propagated forward in time using a spatially second-order scheme in which artificial diffusion is then added. Alternatively, spatial first-order schemes are often used in which additional diffusion is inherent. In regions where the solution is smooth, some or all of this diffusion is subsequently removed, so the solution there is basically second-order. Where the gradient is large, little or none of the diffusion is removed, so the solution in such regions is first-order. In regions of intermediate gradients, the order of the solution depends on how much of the artificial diffusion is removed. In this way, the FCT technique prevents non-physical extrema from being introduced into the solution. The principle of another high-resolution TVD scheme is similar to the FCT method. These algorithms can ensure that the total variation of the variables does not increase with time, thus no spurious numerical oscillations are generated. The solution can be second- or even third-order accurate in the smooth parts of the solution, but only first-order near regions with large gradients.

Comparisons of some numerical advection algorithms have been performed for different test problems, see e.g. [11–14]. In this paper we intend to consider a series of the most frequently used numerical schemes, especially including high-resolution schemes. We test these numerical methods with respect to convectively dominated problems. Numerical diffusivity, production of spurious oscillations, computational efficiency and suitability for grid size or magnitude of diffusion are all taken into account, thus we hope to gain some balanced view on the properties of different schemes in convection–diffusion problems.

In Section 2 a series of numerical methods: traditional first-order upstream, Lax–Friedrichs; second-order upstream, central difference, Lax–Wendroff, Beam–Warming, Fromm; third-order QUICK, QUICKEST schemes and high-resolution FCT and TVD schemes are summarized. In Section 3 numerical results obtained by employing these difference schemes are compared for a pure convection problem with discontinuous initial data, a convection–diffusion problem with sinusoidally shaped initial distribution of the variables as well as for the deformation of the temperature profiles in upwelling and downwelling areas in lakes. Some concluding remarks are given in Section 4.

2. A SERIES OF NUMERICAL METHODS

For simplicity we consider the one-dimensional equation

$$\frac{\partial c}{\partial t}+\frac{\partial f(c)}{\partial x}=\frac{\partial}{\partial x}\left(\Gamma\frac{\partial c}{\partial x}\right) \quad \text{or} \quad \frac{\partial c}{\partial t}+a(c)\frac{\partial c}{\partial x}=\frac{\partial}{\partial x}\left(\Gamma\frac{\partial c}{\partial x}\right) \tag{1}$$

together with appropriate initial and boundary conditions. Here, $a(c) = \partial f(c)/\partial c$ is the characteristic (convective) speed depending on the variable c, Γ may be a turbulent diffusion coefficient and c may either be the concentration of a passive tracer, the temperature, salinity or a velocity component.

It is worthwhile to mention that depending on the values of a and Γ, (1) changes its character. If $a = 0$ and $\Gamma \neq 0$, (1) is parabolic, but is hyperbolic when $a \neq 0$ and $\Gamma = 0$. If a, Γ are functions of x and t, the character may change locally and with time.

The numerical treatment of a convection–diffusion equation involves specific difficulties, which mainly originate form the different scales of the convective and turbulent motion. We will see that for pure diffusion (parabolic equation) or physical diffusively dominated problems, a spatial central and temporal Euler forward difference scheme is suitable, but for convectively dominated problems, difference schemes of convection terms are quite sensible to stability and accuracy. The high discretization error of finite difference techniques lead often to physically unrealistic results. Apart from numerical instabilities, fundamental mechanical or thermodynamical principles can be violated. Fronts will not be sufficiently resolved due to numerical diffusion [15].

Integrating (1) over the rectangle $[x_{j-1/2}, x_{j+1/2}] \times [t^n, t^{n+1}]$ and introducing the definitions of the spatial and temporal mean values

$$U_j^n = \frac{1}{\Delta x} \int_{x_{j-1/2}}^{x_{j+1/2}} c(x, t^n)\, \mathrm{d}x, \qquad \mathscr{F}_{j+1/2} = \mathscr{F}(U;\ j+1/2) = \frac{1}{\Delta t} \int_{t^n}^{t^{n+1}} f(x_{j+1/2}, t)\, \mathrm{d}t,$$
$$\mathscr{D}_{j+1/2} = \mathscr{D}(U;\ j+1/2) = \frac{1}{\Delta t} \int_{t^n}^{t^{n+1}} \left(\Gamma \frac{\partial c}{\partial x}\right)(x_{j+1/2}, t)\, \mathrm{d}t \tag{2}$$

a difference equation in form of

$$U_j^{n+1} = U_j^n - \frac{\Delta t}{\Delta x} \{\mathscr{F}_{j+1/2} - \mathscr{F}_{j-1/2}\} + \frac{\Delta t}{\Delta x} \{\mathscr{D}_{j+1/2} - \mathscr{D}_{j-1/2}\} \tag{3}$$

is obtained in which lower case subscripts j denote the grid points while upper case superscripts n indicate the time step. $\mathscr{F}_{j\pm1/2}$ denote the convection fluxes and $\mathscr{D}_{j\pm1/2}$ indicate the diffusion fluxes on the cell boundaries at $x_{j\pm1/2}$ respectively, which are functions of the cell averages of the neighbouring cells. These numerical fluxes may have different forms depending on the order of accuracy and types of interpolation. If the cell averages in the flux function are taken at the time level t^n, one obtains an explicit numerical scheme, whilst using cell averages at time t^{n+1} results in an implicit method.

The most rudimentary argument about using the flux (or conservative) form (3) rather than the advective from to model the transport of the physical variable is that with the flux form it is simpler to assure that total physical variable is conserved. This is particularly so for a no-flux boundary condition. It has also been argued that by using the flux form it is easier to avoid the numerical non-linear instabilities of the type reported by [16].

2.1. Central difference scheme (CDS)

A CDS in space for both the convection and the diffusion terms in the forms of

$$\mathscr{F}_{j+1/2} = f(U_{j+1/2}), \qquad \mathscr{D}_{j+1/2} = \Gamma_{j+1/2}\frac{U_{j+1} - U_j}{\Delta x}, \quad \text{with } U_{j+1/2} = \frac{1}{2}(U_j + U_{j+1}) \tag{4}$$

and a leap frog time step with reference only to the convection term as well as an Euler forward temporal scheme regarding the diffusion term are suggested, i.e.

$$U_j^{n+1} = U_j^{n-1} - \frac{2\Delta t}{\Delta x}(\mathscr{F}_{j+1/2}^n - \mathscr{F}_{j-1/2}^n) + \frac{2\Delta t}{(\Delta x)^2}(\Gamma_{j+1/2}^{n-1}(U_{j+1}^{n-1} - U_j^{n-1}) - \Gamma_{j-1/2}^{n-1}(U_j^{n-1} - U_{j-1}^{n-1})) \tag{5}$$

That the discretizations of the convection and the diffusion terms are considered at different time levels is because, for a central difference scheme in space, the leap frog time step is always unstable when $a = 0$ (pure diffusion case) while the Euler forward scheme in time results in numerical instability for a pure convection problem ($\Gamma = 0$). Therefore, the discretization (5) ensures numerical stability for the convection–diffusion problem both with dominant convection effect with prevailing diffusion term.

However, for difference scheme (5), if the grid Péclet number (or cell Reynolds number) defined by

$$Pe = a\Delta x/\Gamma \tag{6}$$

exceeds the critical value $Pe = 2$, e.g. the convection term is dominant, oscillatory grid dispersion may occur [17], which is unphysical. In order to avoid the above problems Pe must be made smaller by using a finer spacing. This can become very costly in terms of computer time. Another remedy is to add large artificial diffusion, but that would make the original problem unrealistic.

2.2. Upstream difference scheme (UDS)

The above emerging numerical oscillations in the CDS are due to an unphysical CDS for the convection term, because at any spatial point information by convection can be coming only from the upstream direction of this point. In order to avoid the above problem, non-centred UDSs in space for the convection term may be used. But as we shall see, this introduces alternative difficulties.

Because for most flows of practical interest, the classical, second-order central scheme for diffusion terms is entirely adequate, from now on, we will discuss different difference schemes only mainly for convection terms. If one considers only the convective part of (1) the equation is the simplest first-order hyperbolic equation

$$\frac{\partial c}{\partial t}+\frac{\partial f(c)}{\partial x}=0 \quad \text{or} \quad \frac{\partial c}{\partial t}+a(c)\frac{\partial c}{\partial x}=0 \tag{7}$$

It has the general solution $c=f(x-at)$ if $a=$ constant, where $f(x)$ is an arbitrary function depending on the initial condition. The lines $x-at$ are called characteristics, and c is constant on these lines. With this in mind a difference scheme is constructed which depends on the slope of the characteristics, i.e. depends on the sign of a. The new value U_j^{n+1} is computed by tracing the characteristic passing through U_j^{n+1} back to the previous time level where the solution can be computed by linear interpolation from neighbouring grid points. More details are given in [18].

With the expression of the convection flux

$$\mathscr{F}_{j+1/2}^n=\begin{cases} f(U_j^n) & \text{for } a_{j+1/2}^n>0 \\ f(U_{j+1}^n) & \text{for } a_{j+1/2}^n<0 \end{cases} \tag{8}$$

a first-order accurate upstream scheme of (1) can be written as follows [19]:

$$U_j^{n+1}=U_j^n-\frac{\Delta t}{2\Delta x}\{f_{j+1}^n-f_{j-1}^n-|a_{j+1/2}^n|\Delta U_{j+1/2}^n+|a_{j-1/2}^n|\Delta U_{j-1/2}^n\} \tag{9}$$

in which $\Delta U_{j+1/2}^n=U_{j+1}^n-U_j^n$, $f_j^n=f(U_j^n)$. The characteristic speed $a_{j+1/2}^n$ is defined by using the Rankine–Hugoniot jump condition [20]

$$a_{j+1/2}^n=\begin{cases} (f_{j+1}^n-f_j^n)/\Delta U_{j+1/2}^n, & \Delta U_{j+1/2}^n\neq 0 \\ a(U_j^n), & \Delta U_{j+1/2}^n=0 \end{cases} \tag{10}$$

The difference equation (9) can be seen as a three-point central difference method plus a numerical viscosity term, i.e. with the fluxes at the cell interfaces

$$\mathscr{F}_{j+1/2}^n=\frac{1}{2}(f_{j+1}^n+f_j^n-\phi_{j+1/2}^n), \qquad \phi_{j+1/2}^n=|a_{j+1/2}^n|\Delta U_{j+1/2}^n \tag{11}$$

which indicates that the UDS for the convection term is equivalent to the CDS for this term and an additional numerical diffusion term

$$\frac{\partial c}{\partial t}+a\frac{\partial c}{\partial x}=\frac{\partial}{\partial x}\left(\Gamma_{\text{num}}\frac{\partial c}{\partial x}\right), \quad \text{with } \Gamma_{\text{num}}=|a|\Delta x/2 \tag{12}$$

Similar problems as oscillations in numerical solutions discussed in the last subsection with central difference may not be encountered, thus such one-sided upstream differences are not restricted by that kind of criteria of the Péclet number ($Pe<2$) but such schemes lead to large numerical diffusion in time-dependent problems.

2.3. Lax–Friedrichs scheme

Another example of first-order finite difference approximations is the Lax–Friedrichs scheme of the form

$$U_j^{n+1} = \frac{1}{2}(U_{j+1}^n + U_{j-1}^n) - \frac{\Delta t}{2\Delta x}(f_{j+1}^n - f_{j-1}^n) \tag{13}$$

It can be seen as a scheme with the fluxes at the interfaces

$$\mathscr{F}_{j+1/2}^n = \frac{1}{2}\left\{ f_{j+1}^n + f_j^n - \frac{\Delta x}{\Delta t}(U_{j+1}^n - U_j^n) \right\} \tag{14}$$

As in the upstream method (11), the Lax–Friedrichs method also has an numerical dissipation term $\phi_{j+1/2}^{\mathrm{LF}} = (\Delta x/\Delta t)\Delta U_{j+1/2}^n$ corresponding to a diffusion coefficient of $\Gamma_{\mathrm{num}} = (\Delta x)^2/(2\Delta t)$.

2.4. Second-order upstream scheme (2UDS) and Fromm's method

The upstream difference scheme (9) possesses only first-order accuracy in space. By using Taylor series expansion in space, the value at the interface $x_{j+1/2}$ can be written as

$$U_{j+1/2} = c(x_j + \Delta x/2, t) = c(x_j, t) + \frac{1}{2}\Delta x \frac{\partial c}{\partial x} + \frac{1}{8}(\Delta x)^2 \frac{\partial^2 c}{\partial x^2} + \cdots \tag{15}$$

By retaining only the first two terms of (15) and using an upstream difference approximation for the appearing spatial derivative, (15) becomes

$$U_{j+1/2}^n = \frac{3}{2}U_j^n - \frac{1}{2}U_{j-1}^n, \qquad a_{j+1/2}^n > 0 \tag{16}$$

representing a linear extrapolation from U_{j-1}^n through U_j^n. If $a_{j+1/2}^n < 0$, the value at the interface is

$$U_{j+1/2}^n = \frac{3}{2}U_{j+1}^n - \frac{1}{2}U_{j+2}^n, \qquad a_{j+1/2}^n < 0 \tag{17}$$

Equations (16) and (17) are conveniently implemented as follows:

$$\begin{aligned} U_{j+1/2}^n = {} & \frac{1}{2}(U_{j+1}^n + U_j^n) - \frac{1}{4}(U_{j+2}^n - U_{j+1}^n - U_j^n + U_{j-1}^n) \\ & + \frac{1}{4}\operatorname{sgn}(a_{j+1/2}^n)(U_{j+2}^n - 3U_{j+1}^n + 3U_j^n - U_{j-1}^n) \end{aligned} \tag{18}$$

Substituting (18) into (3) with $\mathscr{F}_{j+1/2} = f(U_{j+1/2})$, the corresponding difference equation for the upstream scheme can be obtained.

Formm's method [21] results from averaging the values of the second-order central and second-order upstream schemes. The interpolant is linear but dependent on the velocity direction. Then, the value at the interface has the form

$$U^n_{j+1/2} = \begin{cases} U^n_j + \dfrac{1}{4}(U^n_{j+1} - U^n_{j-1}), & a^n_{j+1/2} > 0 \\ U^n_{j+1} - \dfrac{1}{4}(U^n_{j+2} - U^n_j), & a^n_{j+1/2} < 0 \end{cases} \tag{19}$$

2.5. QUICK scheme

The quadratic upstream interpolation for convective kinematics (QUICK) scheme stems from a velocity direction-dependent piecewise-parabolic interpolation. By retaining the first three terms of (15) and using upstream-weighted central difference approximations for the derivatives appearing there, the estimated interface value is

$$U^n_{j+1/2} = \begin{cases} U^n_j + \dfrac{1}{4}(U^n_{j+1} - U^n_{j-1}) + \dfrac{1}{8}(U^n_{j+1} - 2U^n_j + U^n_{j-1}) & \text{for } a^n_{j+1/2} > 0 \\ U^n_{j+1} - \dfrac{1}{4}(U^n_{j+2} - U^n_j) + \dfrac{1}{8}(U^n_{j+2} - 2U^n_{j+1} + U^n_j) & \text{for } a^n_{j+1/2} < 0 \end{cases} \tag{20}$$

We could generalize CDS (4), second-order upstream scheme (16), Fromm's scheme (19) and QUICK (20) by writing

$$U^n_{j+1/2} = \frac{1}{2}(U^n_{j+1} + U^n_j) - \mathscr{CF}(U^n_{j+1} - 2U^n_j + U^n_{j-1}) \quad \text{for } a^n_{j+1/2} > 0 \tag{21}$$

and similarly for $a^n_{j+1/2} < 0$, introducing a 'curvature-factor' coefficient, $\mathscr{CF}$. For the second-order central scheme, $\mathscr{CF} = 0$; for second-order upstream; $\mathscr{CF} = 1/2$; for Formm's method, $\mathscr{CF} = 1/4$; and for QUICK method, $\mathscr{CF} = 1/8$. Such schemes are at least second-order accurate – and third-order accurate for $\mathscr{CF} = 1/8$ [22].

The value at the right interface of these high-order spatial difference schemes is implemented for any sign of $a^n_{j+1/2}$ as follows:

$$\begin{aligned} U^n_{j+1/2} = {} & \frac{1}{2}(U^n_{j+1} + U^n_j) - \frac{\mathscr{CF}}{2}(U^n_{j+2} - U^n_{j+1} - U^n_j + U^n_{j-1}) \\ & + \frac{\mathscr{CF}}{2}\operatorname{sgn}(a^n_{j+1/2})(U^n_{j+2} - 3U^n_{j+1} + 3U^n_j - U^n_{j-1}) \end{aligned} \tag{22}$$

In unsteady flows that are primarily convective, field variations are carried along at the local fluid velocity. A better streaming estimation procedure can be used in conjunction with quadratic upstream interpolation. Such a method was developed by Leonard [11], named QUICKEST (QUICK with estimated streaming terms). It is third-order accurate in space as the QUICK scheme, and second-order in time. For brevity we do not here repeat this method, but will only demonstrate some numerical results for it.

2.6. Lax–Wendroff and Beam–Warming schemes

A wide variety of methods can be devised for the convection equation by using different finite difference approximations. Most of these are based directly on finite difference approximations or Taylor series expansion in space. The Lax–Wendroff method [23] is based on Taylor series expansion in time

$$c(x, t+\Delta t) = c(x, t) + \Delta t \frac{\partial c}{\partial t} + \frac{1}{2}(\Delta t)^2 \frac{\partial^2 c}{\partial t^2} + \cdots = c(x, t) - a\Delta t \frac{\partial c}{\partial x} + \frac{1}{2} a^2 (\Delta t)^2 \frac{\partial^2 c}{\partial x^2} + \cdots \tag{23}$$

where the convection equation (7) has been used. The Lax–Wendroff method then results from retaining only the first three terms of (23) and using centered difference approximations for the derivatives appearing there

$$U_j^{n+1} = U_j^n - \frac{a\Delta t}{2\Delta x}(U_{j+1}^n - U_{j-1}^n) + \frac{(a\Delta t)^2}{2(\Delta x)^2}(U_{j+1}^n - 2U_j^n + U_{j-1}^n) \tag{24}$$

The Beam–Warming method is a one-sided version of Lax–Wendroff. It is also obtained from (23), but now using second-order accurate one-sided approximations of the derivatives

$$U_j^{n+1} = U_j^n - \frac{a\Delta t}{2\Delta x}(3U_j^n - 4U_{j-1}^n + U_{j-2}^n) + \frac{(a\Delta t)^2}{2(\Delta x)^2}(U_j^n - 2U_{j-1}^n + U_{j-2}^n) \tag{25}$$

Both the Lax–Wendroff and the Beam–Warming schemes are of second-order accuracy not only in space but also in time.

2.7. Flux corrected transport

As has been indicated and will also be seen in numerical results, for problems with convection terms, traditional high-order accuracy methods (e.g. CDS, 2UDS, Lax–Wendroff, etc.) result in unexpected oscillations near zones with steep gradients in the variables, while the first-order upstream differencing scheme (UDS, Lax–Friedrichs) displays a large false diffusion, and there is no way of suppressing numerical diffusion and simultaneously having the desired accuracy except for reducing spatial grid sizes which causes large computer time. Therefore, it seems quite reasonable to try to add some *anti-diffusion* to the schemes that balance the unwanted numerical diffusion. Boris and Book [1] and Book *et al.* [2,3] offer such a method and call it FCT technique. The FCT strategy is to add as much of this anti-diffusive flux as

possible without increasing the variation of the solution, to ensure at least second-order accuracy on smooth solutions and yet give well-resolved non-oscillatory discontinuities.

The method consists of the following steps: (i), one uses one of the traditional schemes (e.g. first-order UDS, Lax–Friedrichs or second-order CDS, 2UDS, Lax–Wendroff, Beam–Warming, etc.), and adds artificial diffusion where necessary (e.g. for second-order schemes) so to reach positiveness and, (ii) one eliminates false diffusion $\tilde{\Gamma}$ added to high-order schemes (e.g. CDS), or which was inherent in the scheme (e.g. first-order UDS). In principle the second step is of the form

$$\frac{\partial c}{\partial t} = -\frac{\partial}{\partial x}\left(\tilde{\Gamma}\frac{\partial c}{\partial x}\right) \tag{26}$$

where $\tilde{\Gamma}$ denotes the diffusive coefficient which is added artificially or is inherent in the traditional schemes in the first step.

This anti-diffusion can be discretized from time level n to $n+1$ in the form

$$U_j^{n+1} = U_j^n - \frac{\Delta t}{(\Delta x)^2}(\mathscr{A}_{j+1/2}^n - \mathscr{A}_{j-1/2}^n) \tag{27}$$

where $\mathscr{A}$ is the *corrected* anti-diffusive flux, which eliminates the excessive numerical diffusion where it is possible. Since additional viscosity is typically needed only near discontinuities and large gradients, the coefficient of this anti-diffusive flux might also depend on the behaviour of the solution, being smaller near discontinuities and steep gradients than in smooth regions.

The $\mathscr{A}$ may be considered as a flux which is successively added and subtracted, thus satisfying conservation conditions. However, positiveness cannot be warranted. To achieve positiveness and avoid formation of new maxima and minima with the transported and diffused solution, a limiter for the anti-diffusive flux is introduced

$$\mathscr{A}_{j+1/2}^n = \tilde{\Gamma}_{j+1/2}^n S_{j+1/2}^n \max[0,\ \min(|U_{j+1}^n - U_j^n|,\ S_{j+1/2}^n(U_j^n - U_{j-1}^n),\ S_{j+1/2}^n(U_{j+2}^n - U_{j-1}^n))] \tag{28}$$

with $S_{j+1/2}^n = \mathrm{sgn}(U_{j+1}^n - U_j^n)$. We can see that this correction depends also on neighbouring values, which become important in case of steep gradients. In case the minimum is equal to $|U_{j+1}^n - U_j^n| \neq 0$, we have $\mathscr{A}_{j+1/2}^n = \tilde{\Gamma}_{j+1/2}^n\ (U_{j+1}^n - U_j^n)$ as the uncorrected anti-diffusive flux. Otherwise, this formation does not permit that local maxima or minima are generated.

For UDS numerical diffusion is inherent. Here, the uncorrected anti-diffusive flux is $\tilde{\Gamma}_{j+1/2} = |a_{j+1/2}^n|\Delta x/2$ as shown in (12). It can be easily seen if this uncorrected anti-diffusive flux is used for FCT, the same numerical results are obtained as for CDS. Therefore, the effect of the limiter (28) is decisive for FCT. In the numerical results below, the FCT scheme always indicates the UDS in the first step plus the FCT in the second step.

A more general limiter especially suitable for explicit multidimensional implementations is described by Zalesak [4].

2.8. Total variation diminishing

Apart from FCT, another so-called high-resolution method is TVD. The concept of TVD schemes was introduced by Harten [7]. For certain types of equations these algorithms can ensure that the sum of the variable variations over the whole computational domain does not increase with time, thus no spurious numerical oscillations are generated. Since by numerical schemes only the value of the cell average is available, with the concept of TVD the cells are reconstructed in the way that no spurious oscillation is present near a discontinuity or a zone with steep gradients and high-order accuracy is retained simultaneously, e.g. the solution can be second- or third-order accurate in the smooth parts of the solution, but the scheme possesses only first-order accuracy at extrema.

As for the FCT method, the main idea behind the TVD method is also to attempt to use a high-order method, but to modify the method and increase the amount of numerical dissipation in, and only in, the neighbourhood of a discontinuity or a steep gradient so that the eventually occurring oscillations in high-order methods are suppressed.

In the TVD method the non-oscillatory requirement is imposed more directly. It requires that

$$\sum_{j=0}^{N-1} \left|U_{j+1}^{n+1} - U_j^{n+1}\right| \leq \sum_{j=0}^{N-1} \left|U_{j+1}^{n} - U_j^{n}\right| \tag{29}$$

The contribution of terms in non-conservative form, e.g. physical source terms, are added separately without the limiting procedures of TVD.

In the upstream method mentioned in Subsection 2.2, the physical value at the cell boundary $U_{j+1/2}$ is assumed to be one of the adjacent cell averages, either U_j or U_{j+1}. This is equivalent to using a piecewise constant approximation over the cell. It then only gives first-order accuracy. In accordance with the TVD condition the distribution of the physical variables over the cell is reconstructed by a linear piecewise reconstruction

$$\tilde{c}^n(x, t_n) = U_j^n + \sigma_j^n(x - x_j), \quad x \in [x_{j-1/2}, x_{j+1/2}] \tag{30}$$

where the slop limiter $\sigma_j = \phi_j(U_{j+1} - U_j)/\Delta x$ and ϕ_j is defined as a function of the ratio of consecutive gradients θ_j

$$\phi_j = \phi(\theta_j), \qquad \theta_j = \frac{U_j - U_{j-1}}{U_{j+1} - U_j} \tag{31}$$

To obtain the second-order accurate cell reconstruction and satisfy the TVD property, $\phi(\theta)$ must satisfy some conditions, i.e. it should be confined to a certain region in the $\phi - \theta$ diagram.

There are various selections for the function $\phi(\theta)$. If $\phi(\theta)$ is defined by the upper boundary of the second-order TVD region, there results the so-called Superbee limiter [24]

$$\phi^{\text{Superbee}}(\theta) = \max(0, \min(1, 2\theta), \ \min(\theta, 2)) \tag{32}$$

while the Minmod limiter

$$\phi^{\text{Minmod}}(\theta) = \max(0, \min(1, \theta)) \tag{33}$$

is obtained if $\phi(\theta)$ is defined by the lower boundary of the second-order TVD region. The Woodward limiter lies between them

$$\phi^{\text{Woodward}}(\theta) = \max(0,\ \min(2, 2\theta, 0.5(1+\theta))) \tag{34}$$

Since $\phi(\theta)$ determines the value of the anti-diffusion flux, different limiters result in different diffusion. The Minmod and Superbee limiters are the most and least diffusive of all acceptable limiters, respectively. The Woodward limiter lies in between.

The application of the slope limiters can eliminate unwanted oscillations and gives second-order accurate reconstruction for the smooth solutions (except near critical points) over the cell. One can therefore develop high-order resolution schemes without spurious oscillation, but with the ability to capture a possible discontinuity.

Consider a linear piecewise reconstruction; there are two values for each interface, i.e. $U^{\mathrm{L}}_{j+1/2}$; $U^{\mathrm{R}}_{j+1/2}$; one stems from the left-side cell U_j, and the other is due to the right-side element, U_{j+1}. They are

$$U^{\mathrm{L}}_{j+1/2} = U_j + \frac{1}{2}\Delta x \sigma_j, \qquad U^{\mathrm{R}}_{j+1/2} = U_{j+1} - \frac{1}{2}\Delta x \sigma_{j+1} \tag{35}$$

We select a few cases of TVD schemes for our tests.

2.8.1. MUSCL schemes. Spatially high-order monotonic upstream schemes for conservation laws (MUSCL) are introduced by applying the first-order upstream numerical flux (11) and replacing the arguments U_j and U_{j+1} by the $U^{\mathrm{L}}_{j+1/2}$ and $U^{\mathrm{R}}_{j+1/2}$ respectively. Since the linear piecewise reconstruction is second-order accurate, the spatially second-order MUSCL scheme is of the form

$$U^{n+1}_j = U^n_j - \frac{\Delta t}{\Delta x}(\mathscr{F}_{j+1/2} - \mathscr{F}_{j-1/2}),$$
$$\text{with } \mathscr{F}_{j+1/2} = \frac{1}{2}\{f(U^{\mathrm{R}}_{j+1/2}) + f(U^{\mathrm{L}}_{j+1/2}) - \phi^{\mathrm{MUSCL}}_{j+1/2}\} \tag{36}$$

where $\phi^{\mathrm{MUSCL}}_{j+1/2} = |a^{\mathrm{RL}}_{j+1/2}|(U^{\mathrm{R}}_{j+1/2} - U^{\mathrm{L}}_{j+1/2})$ is called the dissipative limiter. The characteristic speed $a^{\mathrm{RL}}_{j+1/2}$ is obtained from the Rankine–Hugoniot jump condition

$$a^{\mathrm{RL}}_{j+1/2} = \begin{cases} \dfrac{f(U^{\mathrm{R}}_{j+1/2}) - f(U^{\mathrm{L}}_{j+1/2})}{U^{\mathrm{R}}_{j+1/2} - U^{\mathrm{L}}_{j+1/2}}, & U^{\mathrm{R}}_{j+1/2} \neq U^{\mathrm{L}}_{j+1/2} \\ a(U_{j+1/2}), & U^{\mathrm{R}}_{j+1/2} = U^{\mathrm{L}}_{j+1/2} \end{cases} \tag{37}$$

2.8.2. TVD Lax–Friedrichs (TVDLF) method. A second-order TVDLF scheme can be obtained by replacing U_{j+1} and U_j in the Lax–Friedrichs scheme (14) with the second-order accurate $U^{\mathrm{R}}_{j+1/2}$ and $U^{\mathrm{L}}_{j+1/2}$

$$U_j^{n+1} = U_j^n - \frac{\Delta t}{\Delta x}\,(\mathscr{F}_{j+1/2} - \mathscr{F}_{j-1/2}) \tag{38}$$

where the fluxes are given by

$$\mathscr{F}_{j+1/2} = \frac{1}{2}\,(f(U^{\mathrm{R}}_{j+1/2}) + f(U^{\mathrm{L}}_{j+1/2}) - \phi^{\mathrm{TVDLF}}_{j+1/2}) \tag{39}$$

with the dissipative limiter

$$\phi^{\mathrm{TVDLF}}_{j+1/2} = \frac{\Delta x}{\Delta t}\,\Delta U^{\mathrm{RL}}_{j+1/2} \tag{40}$$

where $\Delta U^{\mathrm{RL}}_{j+1/2} = U^{\mathrm{R}}_{j+1/2} - U^{\mathrm{L}}_{j+1/2}$. However, this dissipative limiter leads to a very diffusive scheme. Tóth and Odstrčil [14] suggested that the dissipative limiter should be multiplied by the maximum Courant number $C^{\max}_{j+1/2} = |a_{j+1/2}|^{\max}\ \Delta t/\Delta x$ to obtain a modified dissipative limiter

$$\phi^{\mathrm{MTVDLF}}_{j+1/2} = C^{\max}_{j+1}\phi^{\mathrm{TVDLF}}_{j+1/2} = |a_{j+1/2}|^{\max}\Delta U^{\mathrm{RL}}_{j+1/2} \tag{41}$$

which preserves most of the desired properties of a TVD scheme. This scheme is called the modified TVD Lax–Friedrichs method (MTVDLF). Cockburn *et al.* [25] took $|a_{j+1/2}|^{\max} = \max[|a_{j+1/2}(U^{\mathrm{R}}_{j+1/2})|, |a_{j+1/2}(U^{\mathrm{L}}_{j+1/2})|]$. It can be easily seen that for one-dimensional problems with constant convection velocity both MTVDLF and MUSCL scheme are identical.

3. COMPARISONS OF SOME NUMERICAL RESULTS

In this section we present numerical results depicting various numerical schemes listed in the previous section with respect to several simple test problems.

3.1. A convection problem—travelling shock wave

One of the simplest model problems is the one-dimensional convection at constant velocity of an initial data with step function in the variable c without physical diffusion. It has the general solution $c = f(x-at)$, where $f(x)$ is the initial distribution of c assumed by

$$f(x) = \begin{cases} 1, & x \le 0.1 \\ 0, & x > 0.1 \end{cases} \tag{42}$$

The solution describes a wave propagating in the positive x-direction with the velocity a (if $a > 0$). Since the analytic solution is known in this simple case, the numerical solution can be critically evaluated. Varying velocity fields, multidimensions, and non-rectangular co-ordinate systems all increase the difficulties in modelling convection problems, but if an algorithm cannot model this simple problem correctly, then it will be of little use in more complex situations.

We choose the dimensionless convection velocity $a = 0.01$, the grid size $\Delta x = 0.005$ (corresponding to a grid number $N = 200$ for the domain $x \in [0, 1]$). Because the numerical schemes listed in Section 2 are of first-order or second-order accuracy in time respectively, and our main interest is in various spatial difference schemes for the convection term, then in order to avoid numerical error due to discretization in time as far as possible, in the computations we choose a very small time step size $\Delta t = 0.005$. Then, the Courant number $C = a\Delta t/\Delta x = 0.01$ is much smaller than required by stable conditions for many schemes, but not every, $C < 1$.

In Figure 1 the results of using various difference schemes are shown for a dimensionless time $t = 50$, at this time point the jump is moving through $x = 0.6$ from its initial position $x = 0.1$. The highly diffusive nature of the first-order upstream and the Lax–Friedrichs schemes (Figure 1(a) and (b)) are clearly seen due to inherent numerical diffusion. Especially for the Lax–Friedrichs scheme the jump is strongly smeared. For both schemes reducing the grid size Δx (increasing grid number N) will reduce numerical diffusion, but with larger computational time.

Standard second- or higher-order difference methods, e.g. central, Lax–Wendroff, second-order upstream, Beam–Warming, Fromm, QUICK, QUICKEST schemes, eliminate such numerical diffusion but introduce dispersive effects that lead to unphysical oscillations in the numerical solution (Figure 1(c)–(i)). The central and Lax–Wendroff difference schemes introduce propagating numerical dispersion terms (odd-order derivatives) which corrupt large regions of the flow with unphysical oscillations, which are behind the advancing front and damped with the distance to the front. The second upstream and Beam–Warming schemes have been successful in eliminating artificial diffusion, while minimizing numerical dispersion. Their leading truncation errors are (potentially oscillatory) third-order derivative terms. The damped oscillations before the advancing front are typical of these second-order upstream difference methods; however, the fourth-derivative numerical dissipation is large enough to dampen short-wavelength components of the dispersion to some extent. Third-order upstream schemes, e.g. QUICK and QUICKEST, have a leading fourth-derivative truncation error term which is dissipative, but higher-order dispersion terms can still cause overshoots and a few oscillations when excited by nearly discontinuous behaviour of the advected variable, but they are considerably smaller than the other second-order schemes. The profiles simulated by the QUICK and QUICKEST scheme remain comparatively sharp; the small undershoots and overshoots which develop are each about only 5 per cent of the step height, while for the central and the Lax–Wendroff schemes such under- and overshoots can reach almost 30 per cent of the step height; and the ranges of oscillations by the QUICK and QUICKEST schemes are also much smaller than that with the second-order schemes.

For high-resolution methods, e.g. FCT and TVDLF, no oscillations occur in numerical solutions, but visible smearings do still exist although they are much smaller than for the first-order methods. The MTVDLF scheme, which is identical with the MUSCL scheme for

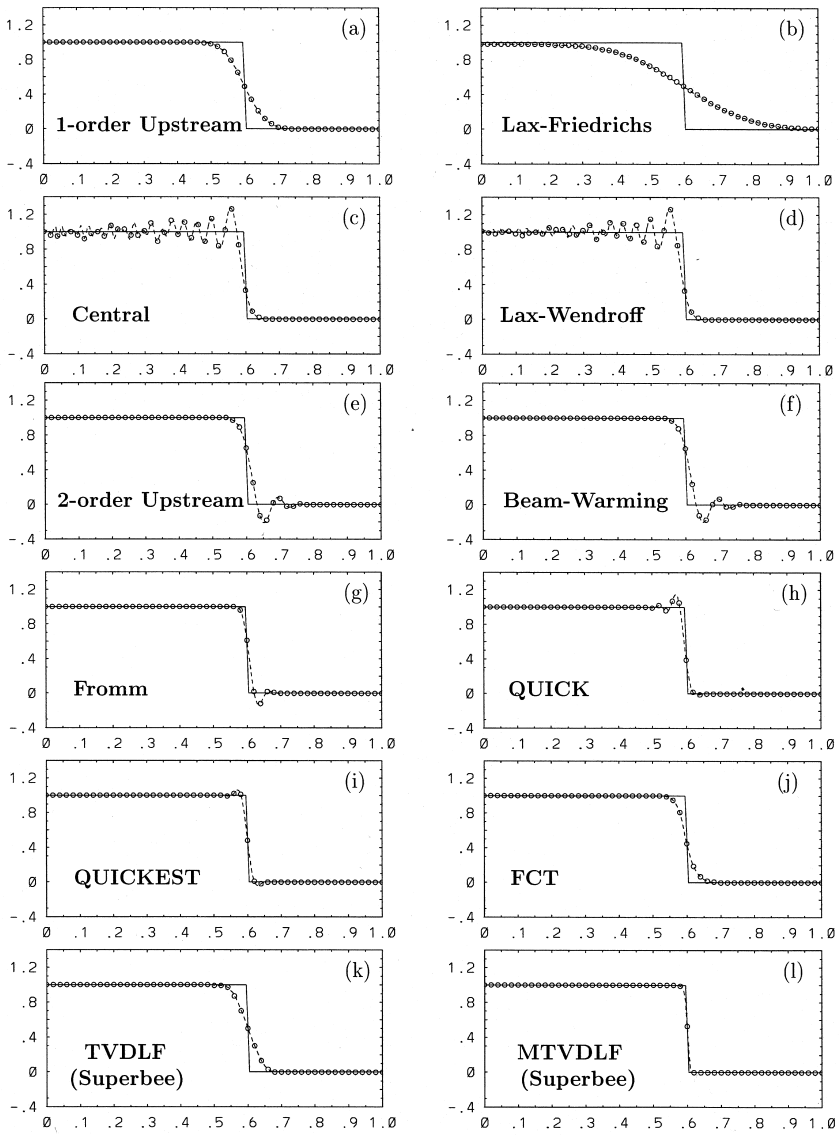

Figure 1. Comparison of different numerical methods with regard to the convective problem with discontinuous initial data. The computations are performed with the grid number $N = 200$, the dimensionless convective velocity $a = 0.01$ and the dimensionless time step $\Delta t = 0.005$. The results are illustrated for the dimensionless time $t = 50$. Solid lines indicate exact solutions; dashed lines are numerical solutions where circles denote the numerical results at every fourth grid point.

this problem, indicates the best agreement with the exact solution of this problem. If the Superbee slope limiter, which possesses the least diffusion of all acceptable limiters, is replaced by the Woodward or Minmod limiters, a little visible diffusion occurs, as seen in Figure 2.

To quantitatively discriminate how well these schemes can describe the convection problem with a discontinuity an error measure for the physical variable c is introduced,

$$\text{Error} = \frac{\sum_j |U_j - c_j^{\text{exact}}|}{\sum_j c_j^{\text{exact}}} \tag{43}$$

where c_j^{exact} denotes the exact solution of the jth cell, while U_j is the corresponding numerical value.

The errors of various difference schemes are listed in Table I with different grid numbers N. It can be seen that the errors decrease with increasing grid number for all numerical schemes, not only for the first-order schemes with numerical diffusion but also for high-order schemes with unphysical oscillations. Therefore, in principle, grid refinement can alleviate these numerical errors, the necessary degree of refinement is often totally impracticable for engineering purposes, especially if one is attempting to model problems as unsteady three-dimensional turbulent flow in lake dynamics. It is worthwhile to mention that the numerical solution of the TVDLF method for small grid number (e.g. $N = 30$ or 50) has even much larger error (numerical diffusion) than that of the first-order upstream scheme; the reason is the property of the Lax–Friedrichs scheme, whose error is proportional to $(\Delta x)^2$. Therefore, in general, one should abandon the TVDLF method, but use the MTVDLF or MUSCL schemes. It is also interesting to note that the third-order QUICK and QUICKEST schemes may produce more inaccurate results than most first-order or second-order difference schemes if spatial resolution is too rough as for the case of $N = 30$. This is the reason that simply going to high-order schemes does not necessarily produce a proportionate increase in accuracy. Among some traditional second-order schemes, although their errors are of the same order as MTVDLF in some cases, but due to their property of oscillation the MTVDLF scheme is still most

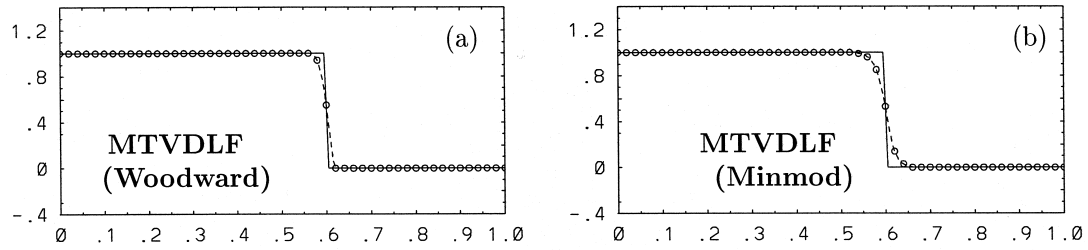

Figure 2. Same as in Figure 1 but here only results are shown for the MTVDLF method with the Woodward and Minmod limiters.

Table I. Errors of the different numerical schemes with regard to the convective problem with discontinuous initial data.

Grid number	$N=30$	$N=50$	$N=100$	$N=200$	$N=400$
Upstream	14.7226	11.7666	8.5956	6.2153	4.4515
Lax–Friedrichs	95.8618	88.5464	58.7152	21.5403	10.0419
Central (CDS)	18.6695	14.8813	10.9839	8.1263	5.9577
Lax–Wendroff	18.5959	14.8037	10.6055	7.3017	4.4946
Two-order upstream	9.3453	7.1468	5.1540	3.6983	2.6897
Beam–Warming	9.3367	7.1317	5.1075	3.5979	2.4665
Fromm	13.4560	4.8806	2.8130	1.7816	1.2093
QUICK	17.6393	7.5005	3.4713	2.1550	1.4496
QUICKEST	16.2218	5.9405	2.7950	1.6164	0.9497
FCT	10.3286	7.5234	4.8463	3.0897	1.9388
TVDLF (Superbee)	82.6425	46.3881	8.5589	4.3027	3.3213
MTVDLF (Superbee)	5.1293	3.1781	1.6370	0.8342	0.4219
MTVDLF (Woodward)	5.6656	3.7669	2.1966	1.3100	0.7975
MTVDLF (Minmod)	7.9639	5.6935	3.6288	2.3241	1.4907

Here results for different spatial resolutions are displayed. The other conditions are the same as in Figure 1.

preferable, because the oscillations resulting from the schemes are of importance, e.g. in the simulation of horizontal propagation of concentration patterns, in many cases leading to locally negative concentrations or other anomalies.

3.2. A convection–diffusion problem

The second type of model problem to be considered is a one-dimensional constant-coefficient version of (1), in which, besides the convection, physical diffusion is included.

We first consider a simple one-dimensional diffusive problem

$$\frac{\partial c}{\partial t}=\Gamma\frac{\partial^2 c}{\partial x^2},\qquad \Gamma=\text{constant} \tag{44}$$

The general solution of (44) for an arbitrary initial distribution, $c(x,\,t=0)=f(x)$, diffusing in an unbounded space is given by [26]

$$c(x,\,t)=\int_{-\infty}^{\infty}\frac{f(\xi)}{2(\pi\Gamma t)^{1/2}}\exp\left\{-\frac{(x-\xi)^2}{4\Gamma t}\right\}\mathrm{d}\xi \tag{45}$$

Then, the solution for a one-dimensional linear convection–diffusion problem

$$\frac{\partial c}{\partial t}+a\frac{\partial c}{\partial x}=\Gamma\frac{\partial^2 c}{\partial x^2},\quad a=\text{constant},\quad \Gamma=\text{constant} \tag{46}$$

can be given by

$$c(x, t) = \int_{-\infty}^{\infty} \frac{f(\xi)}{2(\pi\Gamma t)^{1/2}} \exp\left\{ -\frac{(x - at - \xi)^2}{4\Gamma t} \right\} d\xi \tag{47}$$

Numerical results will be compared with this analytic solution.

In our numerical simulations, the various difference schemes displayed in Section 2 are used for the convection term, but only a classical central difference scheme for the diffusion term due to its reasonableness for most flows of practical interest. We choose all parameters in a physical reasonable range for computing tracer convection–diffusion problems in lakes, although here we deal still only with one-dimensional problems. The studied domain is 10 km long ($x \in [0, 10]$) to ensure the influence of the boundary conditions negligible. The grid size is $\Delta x = 0.1$ km corresponding to a total grid number $N = 100$. The time step size $\Delta t = 2$ s. Test computations indicate that for any smaller time step size numerical solutions of various difference schemes remain basically unchanged. This means that with this time step size numerical errors are not related to time truncation only, but rather to spatial difference schemes. We assume a constant water velocity $a = 0.04$ m s^{-1} in the positive x-direction (a typical water velocity in lakes) and an initial distribution of tracer concentration.

$$c(x, t = 0) = \begin{cases} 0.4 \sin[(x - 2)\pi] & \text{for } x \in [2, 3] \text{ km} \\ 0 & \text{for all other } x \end{cases} \tag{48}$$

whose maximum is at $x = 2.5$ km. A series of computations are performed for various Péclet number, see definition (6), representing the ratio between convection and diffusion to some extent.

In Figure 3(a)–(j) the numerical solutions (dashed lines with circles) simulated by various schemes and the corresponding analytic solution (solid lines) are illustrated at the time point $t = 30$ h for $Pe \to \infty$ indicating pure convection. Results for the Lax–Friedrichs and TVDLF schemes are not shown, because for both schemes the tracer is dispersed rapidly as a result of large numerical diffusion due to the large grid size, so that the numerical errors for both schemes are almost always larger than 100 per cent. Therefore such numerical schemes hold less practical interest for this problem.

It can be seen that, as in Figure 1 for the moving jump problem, all second-order numerical schemes exhibit numerical oscillations, while the first-order upstream, even the high-resolution FCT schemes are accompanied by large numerical diffusion. The behaviour of both the central and the Lax–Wendroff schemes as well as both the second-order upstream and the Beam–Warming schemes are very similar. The third-order QUICK scheme, especially the QUICK-EST scheme, achieves better numerical results. Among all these schemes, the result accomplished by the high-resolution MTVDLF (or MUSCL) is closest to the exact solution.

If there exists physical diffusion, numerical oscillations caused by high-order numerical schemes can be damped out, partly or even entirely, depending on the magnitude of the Péclet number. In Figure 4 the same results as in Figure 3 are depicted but accompanied by physical diffusion with a diffusion coefficient of $\Gamma = 0.2$ m^2 s^{-1}, corresponding to a Péclet number of $Pe = 20$. Owing to this physical diffusion the numerical oscillations exist now only in fairly narrow regions with large gradients, and their amplitudes are also much smaller than in the

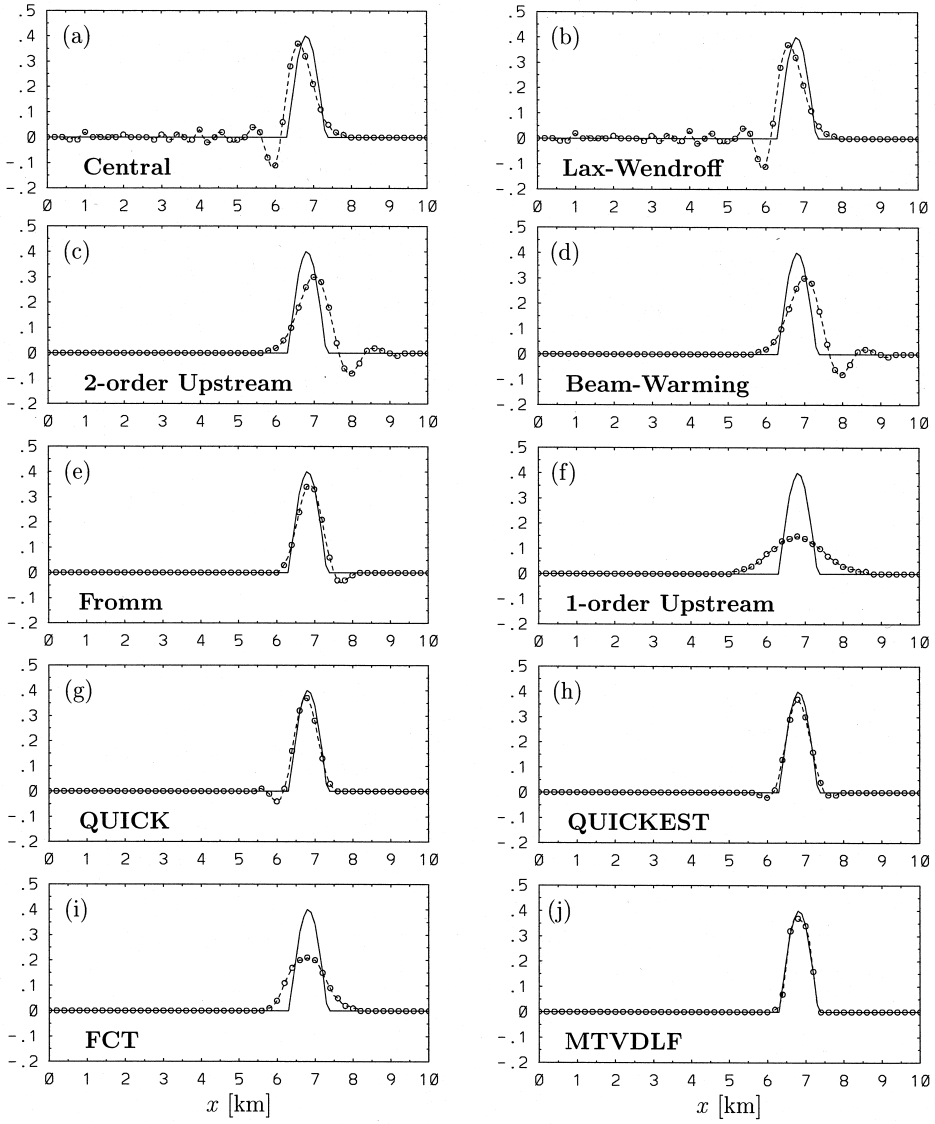

Figure 3. Results of different numerical methods for the tracer convective problem with the initial data of sinusoidal shape in a finite interval [2, 3] km. The computations are performed with the grid number $N = 100$ (corresponding to a grid size of $\Delta x = 100$ m), the convective velocity $a = 0.04$ m s^{-1} and the time step $\Delta t = 2$ s. The results are displayed for the time point $t = 30$ h. Solid lines indicate exact solutions; dashed lines are numerical solutions where circles denote the numerical results at every second grid points.

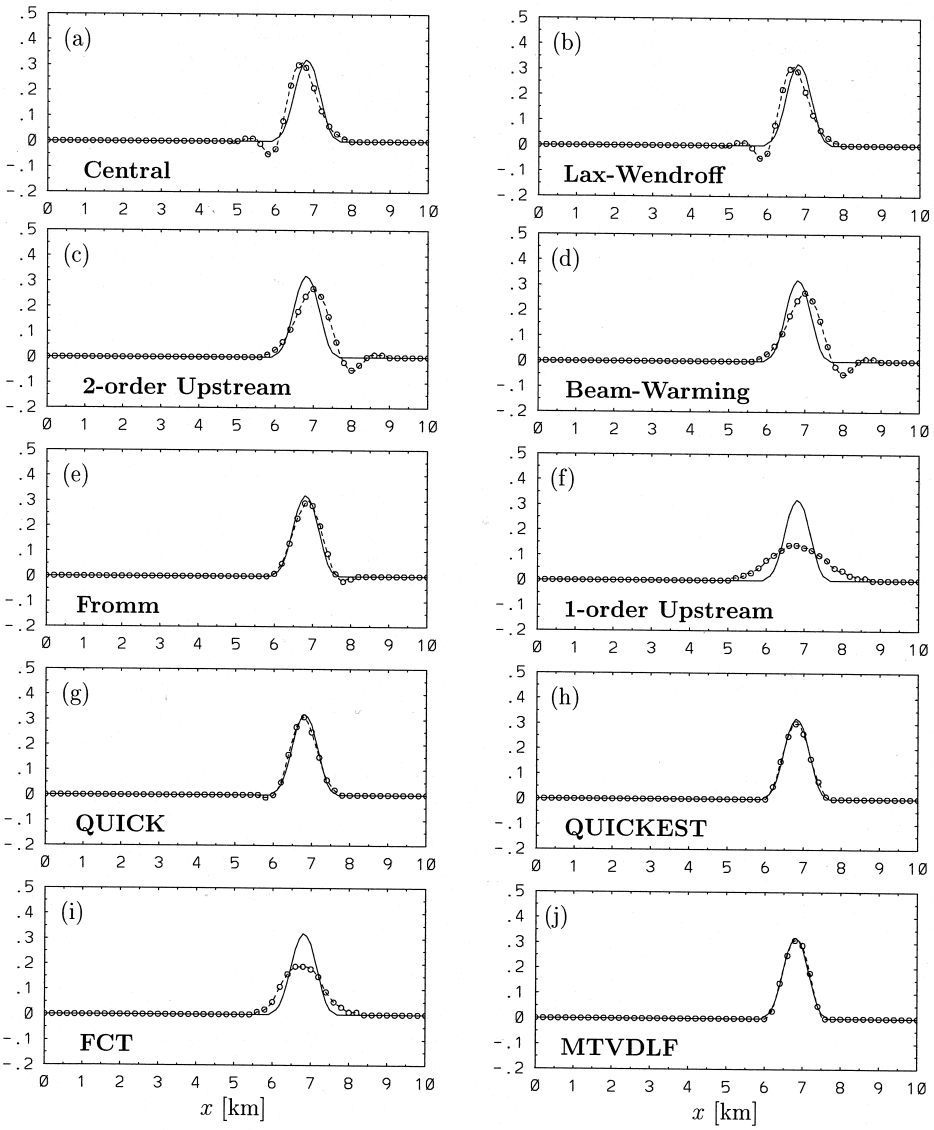

Figure 4. Same as Figure 3 but now for a problem with an additional diffusion term with a diffusion coefficient for $\Gamma = 0.2$ m^2 s^{-1}, corresponding to a Péclet number of $Pe = 20$.

case of pure convection (by comparing with Figure 3). In this case, as the high-resolution MTVDLF scheme, the third-order QUICK and QUICKEST methods produce also fairly good results.

In Table II the computational errors of various difference schemes are listed for different Péclet numbers $Pe = \infty$, 40, 20, 4, 1 and 0.4, which correspond to diffusion coefficients $\Gamma = 0$, 0.1, 0.2, 1, 4 and 10 $m^2\ s^{-1}$ respectively. Obviously, computational errors decrease with decreasing Péclet number. If $Pe < 2$, i.e. the effect of diffusion is dominant in the physical process, the oscillations caused by high-order schemes do no longer occur, the errors of almost all numerical schemes are below 2 per cent, except for the first-order schemes, for which numerical diffusion is still comparable with the physical value. Therefore, oscillatory grid dispersion may be excited only if the Péclet number exceeds the critical value $Pe = 2$, while first-order differences are not restricted by this kind of criteria but such schemes lead to large numerical diffusion.

The differences between the central and Lax–Wendroff as well as between second-order upstream and Beam–Warming schemes are negligibly small, not only for total errors as listen in Table II but also for their local numerical solutions as illustrated in Figures 3 and 4. For the convectively dominated case ($Pe > 20$), the QUICK and QUICKEST schemes are much more inaccurate, although they are even more accurate for large physical diffusion ($Pe \leq 1$) than the MTVDLF scheme with the Superbee limiter. It can also be seen from Table II that the Woodward and Minmod limiters bring fairly large errors into the MTVDLF scheme for large Péclet number due to large numerical diffusion. Among all cases the MTVDLF scheme with the Superbee slope limiter is proved to be most suitable for this physical problem.

3.3. Deformation of temperature profile caused by vertical convection in lakes

As we have seen, for problems with dominant convection terms, conventional high-order accuracy difference methods result in numerical oscillations near steep gradients of variables. Alternatively, first-order difference schemes avoid such oscillations, but inherent numerical diffusion included in such schemes often causes severe inaccuracies. The MTVDLF method seems to be a suitable technique. As another typical illustration of the behaviour of such

Table II. Errors of the different numerical schemes with regard to the convection–diffusion problem with a sinusoidal shape initial data.

Péclet number	$Pe \to \infty$	$Pe = 40$	$Pe = 20$	$Pe = 4$	$Pe = 1$	$Pe = 0.4$
Upstream	102.9591	89.5325	80.0951	46.0459	18.4730	8.4902
Central	86.9377	52.4609	36.8579	7.9801	1.2549	0.5473
Lax–Wendroff	86.2622	52.2619	36.7302	7.9746	1.2526	0.5462
Two-order Upstream	79.3426	62.7262	50.4604	14.7690	2.4435	1.0248
Beam–Warming	79.2177	62.6236	50.3921	14.7508	2.4423	1.0263
Fromm	30.8288	22.2587	16.4414	3.9383	0.6138	0.5434
QUICK	24.1792	16.1582	11.1205	2.1721	0.3260	0.4321
QUICKEST	18.7309	12.1849	8.1762	1.0380	0.0189	0.4022
FCT	69.7538	57.4612	48.5500	18.9875	3.8632	1.3256
MTVDLF (Superbee)	8.0540	6.3105	6.1101	4.7565	1.5656	0.8211
MTVDLF (Woodward)	22.5012	16.7381	12.8656	3.5237	0.5811	0.7144
MTVDLF (Minmod)	51.8834	41.0342	32.9913	10.4607	1.9215	1.1134

Results for different Péclet numbers are displayed. The other conditions are the same as in Figure 3.

schemes, consider the temporal alteration of vertical temperature distributions in a stratified lake.

In a lake the stratification varies seasonally according to as the solar radiation heats the upper most layers of the lake, and wind-induced motions and turbulences transfer this heat to greater depths. By late summer these processes will have established a distinct stratification, that essentially divides the water mass into a warm upper layer (called epilimnion), a cold deep layer (hypolimnion) which are separated by a transition zone (metalimnion) with a sharp temperature gradient. A typical vertical temperature profile for a late summer situation in Alpine lakes is

$$T(z, t=0) = \begin{cases} 17 - 2\exp[(z-20)/5], & 0 \geq z \geq -20 \text{ m} \\ 5 + 10\exp[(-z+20)/5], & z \leq -20 \text{ m} \end{cases} \tag{49}$$

where the vertical co-ordinate z is directed upward with $z = 0$ at the water surface. The largest temperature gradient occurs at depth $z = -20$ m, which is called thermocline. Under the effect of wind stress at the water surface, strong vertical convection, occurring mainly near lake shores, causes a vertical movement and hence declination of the thermocline. Accurate simulation of the temporal alteration of the stratification is decisively important for studying the baroclinic response of a lake.

In lake dynamics the temperature equation (the energy balance) is a three-dimensional convection–diffusion equation. Here, for simplicity, we still only consider one-dimensional motions with a typical vertical velocity of 1.0×10^{-3} m s^{-1} upward (upwelling) and downward (downwelling) respectively; we neglect the effect of diffusion, and choose a time step $\Delta t = 2$ s and a grid size $\Delta z = 2$ m corresponding to a grid number $N = 50$ through the total vertical domain of 100 m. Thus, the hyperbolic variant of (1) for $c = T$ is addressed with (49) as initial condition.

The computed deformations of the temperature profile after 3 days in the presence of upwelling and downwelling respectively, simulated by central differences, are displayed in Figure 5(a). The gradients are smoothed out ahead of the moving frontal interface, while wave-like phenomena appear behind the front. In this example the waves cause numerical oscillations. In many practical computations of lake dynamics such oscillations are so large that physical instability occurs. Therefore, they must be removed by the mechanism for simulating convection that should be incorporated in any model, e.g. by use of a physically reasonable first-order upstream simulation of convection or by adding an artificial diffusion. However, it is clear that in this kind of a model the initially steep temperature gradient will soon be dissipated, as the results show in Figure 5(b) obtained by using the upstream difference scheme. Therefore, removal of the oscillatory effects of the spatial central difference discretization of the convection terms can be accomplished by including sufficient diffusion in the model, but in general this would mean that the numerical diffusion would be far greater than the actual physical diffusion effects. In many cases, such necessary numerical diffusion is so large that numerical results are unrealistic; indeed one can often see in computational lake dynamics that the numerical diffusion is much larger than its physical reasonable value so that some physical interesting phenomena, e.g. internal waves existing everywhere in stratified lakes

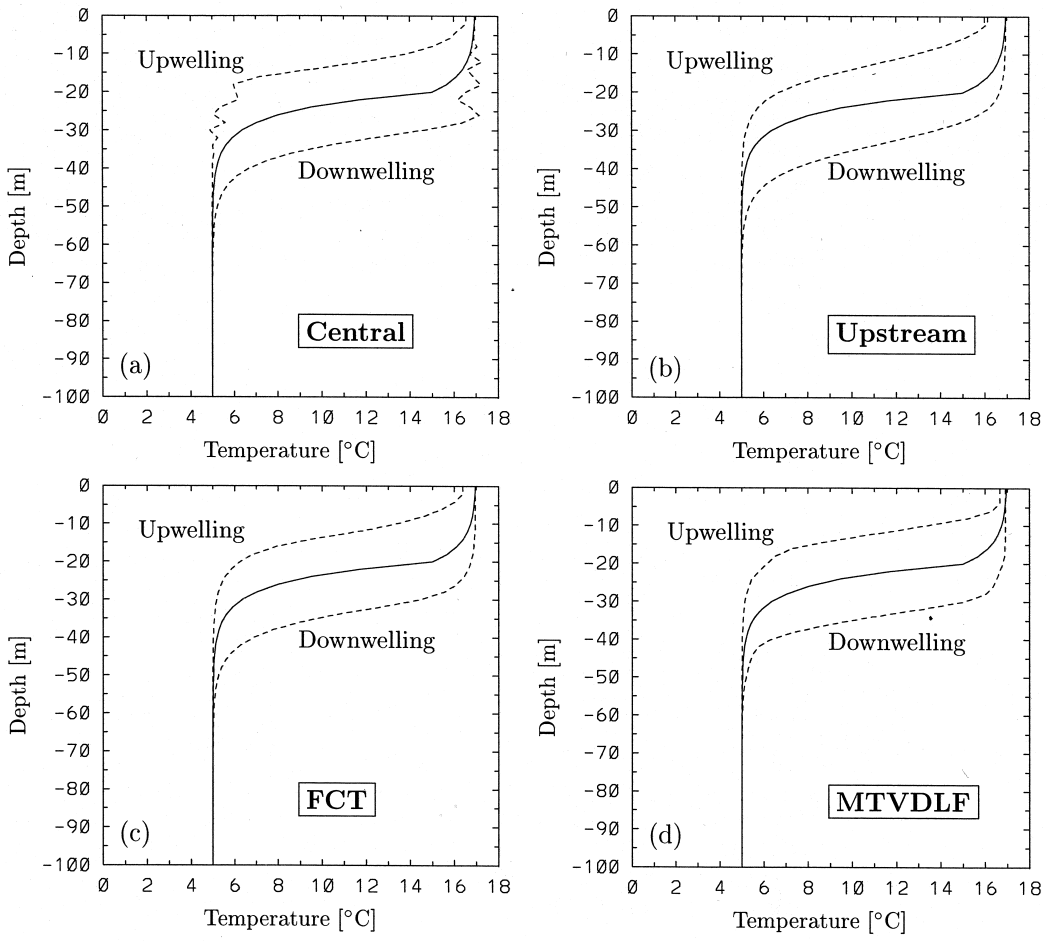

Figure 5. Comparison of different difference schemes on computations of temperature profiles in upwelling and downwelling areas of a lake respectively. Solid lines indicate the initial temperature profile, while dashed lines denote the computed temperature distributions after 3 h in upwelling and downwelling areas with a convection velocity of $\alpha = 1.0 \times 10^{-3}$ m s^{-1} respectively.

are damped out rapidly and not discernible in numerical results. In principle, the required artificial diffusion can always be reduced by increasing the spatial resolution [27], which may become very costly in terms of computer time. As we have seen, attempts have been made to design numerical schemes that can properly deal with convectively dominated problems. A successful way to solve this problem is the use of high-resolution numerical schemes for convection terms. Results are shown in Figure 5(c) using the FCT scheme and in Figure 5(d) for the MTVDLF method. It is obvious by comparison with the upstream scheme (Figure 5(b)) that the FCT scheme reduces the numerical diffusion greatly, but it is still larger than

that obtained by the MTVDLF method with the Superbee limiter and smear is still visible. However, the MTVDLF scheme appears to yield quite accurate result. The temperature profiles simulated with the MTVDLF scheme (Figure 5(d)) are essentially a parallel move of its initial distribution upward (upwelling) and downward (downwelling).

4. CONCLUDING REMARKS

Satisfactory numerical modelling of convection presents a well-known dilemma to the computational fluid dynamicist. On the one hand, traditional second-order differences lead often to unphysical oscillatory behaviour or disastrous non-convergence in regions where convection strongly dominates diffusion. On the other hand, computations based on the classical alternative of first-order, e.g. upstream differencing often suffer from severe inaccuracies due to truncation error. This error mechanism can be associated with equivalent artificial numerical diffusion terms introduced by the first-order upstream differencing of convection. Although, in principle, grid refinement can alleviate all these problems, the necessary degree of refinement is often totally impracticable for engineering purposes. The quadratic upstream interpolation for convective kinematic schemes (QUICK and QUICKEST) has the desirable simultaneous properties of third-order accuracy and inherent numerical convective stability. Compared with traditional first-order or second-order difference schemes, the QUICKEST method can produce a solution of high accuracy, but the methods are clearly limited in their ability to resolve regions of large gradients if spatial resolution is not sufficiently high. With the development of modern numerical modelling, one has step by step found a way out of the dilemma: the use of so-called high-resolution methods. Between two high-resolution methods, the FCT scheme possesses almost no advantage over the QUICK or QUICKEST schemes. The effects of the modified TVDLF method, which is in agreement with the MUSCL scheme in one-dimensional problems, are highly dependent on used slope limiters in some cases. Computations indicate that the MTVDLF scheme with the Superbee slope limiter is most favourable in treating convectively dominated problem.

Although the modified TVDLF schemes can describe convection problems with discontinuity or large gradient very well, they are at most first-order accurate at local extrema. This disadvantage results in the so-called clipping phenomena in some cases, an example of which was illustrated in [10]. To circumvent this, more modern shock-capturing essentially non-oscillatory (ENO) [28,29] and weighted essentially non-oscillatory (WENO) schemes have been introduced [30,31].

In lake and ocean dynamics, with the introduction of three-dimensional circulation models the convection terms take on considerable importance; if not in the equations of motion, then certainly in the temperature and salinity equations. Besides, the interest in hydrodynamic modelling as a tool to study water quality problems led to the use of convection–diffusion equations and their approximate treatment to simulate transports of dissolved or suspended matter in natural basins [32,33]. To our surprise, so far, in computational lake and ocean dynamics, only a few models use high-resolution schemes to simulate convection terms, while more models treat convection terms still only with traditional central or upstream differences. The treatment of convection terms in three-dimensional circulation models in lakes forms the subject of a future publication.

REFERENCES

1. Boris JP, Book DL. Flux-corrected transport I: SHASTA, a fluid transport algorithm that works. *Journal of Computational Physics* 1973; **11**: 38–69.
2. Book DL, Boris JP, Hain K. Flux-corrected transport II: Generalization of the method. *Journal of Computational Physics* 1975; **18**: 248–283.
3. Book DL, Boris JP, Zalesak ST. Flux corrected transport. In *Finite Difference Techniques for Vectorized Fluid Dynamics Circulaitons*, Book DL (ed.). Springer-Verlag: Berlin, 1981; 29–55.
4. Zalesak ST. Fully multidimensional flux-corrected transport algorithms for fluids. *Journal of Computational Physics* 1979; **31**: 335–362.
5. Patnaik G, Guirguis RH, Boris JP, Oran ES. A barely implicit correction for flux-corrected transport. *Journal of Computational Physics* 1987; **71**: 1–20.
6. DeVore CR. Flux-corrected transport techniques for multidimensional compressible magnetohydrodynamics. *Journal of Computational Physics* 1991; **92**: 142–160.
7. Harten A. High resolution schemes for hyperbolic conservation laws. *Journal of Computational Physics* 1983; **49**: 357–393.
8. Nessyahu H, Tadmor E. Non-oscillatory central differencing for hyperbolic conservation laws. *Journal of Computational Physics* 1990; **87**: 408–463.
9. Jiang GS, Tadmor E. Non-oscillatory central schemes for multidimensional hyperbolic conservation laws. *SIAM Journal of Scientific Computing* 1997; **19**(6): 1892–1917.
10. Tai YC. Dynamics of granular avalanches and their simulations with shock-capturing and front-tracking numerical schemes. PhD thesis, Darmstadt University of Technology. Shaker Verlag: Aachen, 2000.
11. Leonard BP. A stable and accurate convective modelling procedure based on quadratic upstream interpolation. *Computer Methods in Applied Mechanics and Engineering* 1979; **19**: 59–98.
12. Chock DP. A comparison of numerical methods for solving the advection equation, II. *Atmosphere and the Environment* 1985; **19**: 571–586.
13. Rood RB. Numerical advection algorithms and their role in atmospheric transport and chemistry models. *Reviews of Geophysica* 1987; **25**(1): 71–100.
14. Tóth G, Odstrčil D. Comparison of some flux corrected transport and total variation diminishing numerical schemes for hydrodynamic and magnetohydrodynamic problems. *Journal of Computational Physics* 1996; **82**: 82–100.
15. Maier-Reimer E. Hydrodynamisch-numerische Untersuchungen zu horizontalen Ausbreitungs- und Transportvorgängen in der Nordsee. Mitt Inst Meerskunde, Uni Hamburg, No. 21, 1973.
16. Phillips NA. An example of nonlinear computational instability. In *The Atmosphere and Sea in Motion*, Bolin B (ed.). Rockefeller Institute Press: New York, 1959; 501–504.
17. Price HS, Varga RS, Warren JE. Application of oscillation matrices to diffusion convection equation. *Journal of Mathematics and Physics* 1966; **45**: 301–311.
18. Mesinger F, Arakawa A. Numerical methods used in atmospheric models. *GARP Publication Series No. 17*, 1976.
19. Huang LC. Pesudo-unsteady difference schemes for discontinuous solution of steady-state, one-dimensional fluid dynamics problems. *Journal of Computational Physics* 1981; **42**: 195–211.
20. Roe PL. Approximate Riemann solvers, parameter vectors, and difference schemes. *Journal of Computational Physics* 1981; **43**: 357–372.
21. Fromm JE. A Method for reducing dispersion in convective difference schemes. *Applied Mathematics Modelling* 1968; **19**(11): 640–653.
22. Leonard BP. Order of accuracy of QUICK and related convection–diffusion schemes. *Appllied Mathematics Modelling* 1995; **19**(11): 640–653.
23. Lax P, Wendroff B. System of conservation laws. *Communications in Pure and Applied Mathematics* 1960; **13**: 217–237.
24. Sweby PK. High resolution schemes using flux limiters for hyperbolic conservation laws. *SIAM Journal of Numerical Analysis* 1984; **21**(5): 995–1101.
25. Cockburn B, Lin SY, Shu CW. TVB Runge–Kutta local projection discontinuous Galerkin finite element method for conservation laws III: one-dimensional systems. *Journal of Computational Physics* 1989; **84**: 90.
26. Carslaw HH, Jaeger JC. *Conduction of Heat in Solids* (2nd edn). Oxford University Press: Oxford, 1959.
27. Wang Y, Hutter K. A semi-implicit semi-spectral primitive equation model for lake circulation dynamics and its stability performance. *Journal of Computational Physics* 1998; **139**: 209–241.
28. LeVeque RJ. *Numerical Methods for Conservation Laws*. Birhäuser Verlag: Basel, 1992.
29. Sonar T. *Mehrdimensionale Eno-Verfahren*. B.G. Teubner: Stuttgart, 1997.

30. Liu X-D, Osher S, Chan T. Weighted essentially non-oscillatory schemes. *Journal of Computational Physics* 1994; **115**: 200–212.
31. Jiang GS, Wu CC. A high-order WENO finite difference scheme for the equations of ideal magnetohydrodynamics. *Journal of Computational Physics* 1999; **150**: 561–594.
32. Lam DCL, Simons TJ. Numerical computations of advective and diffusive transports of chloride in Lake Erie during 1970. *Journal of the Fisheries Research Board of Canada* 1976; **33**: 537–549.
33. Hutter K, Wang Y. The role of advection and stratification in wind-driven diffusion problems of Alpine lakes. *Journal of Lake Sciences* 1998; **10**: 447–475.

